

One and Two Hydrogen Molecules in the Large Cage of the Structure II Clathrate Hydrate: Quantum Translation–Rotation Dynamics Close to the Cage Wall

Francesco Sebastianelli, Minzhong Xu, Dalal K. Kanan, and Zlatko Bačić*

Department of Chemistry, New York University, New York, New York 10003

Received: April 27, 2007

We have performed a rigorous theoretical study of the quantum translation–rotation (T–R) dynamics of one and two H₂ and D₂ molecules confined inside the large hexakaidecahedral (5¹²6⁴) cage of the sII clathrate hydrate. For a single encapsulated H₂ and D₂ molecule, accurate quantum five-dimensional calculations of the T–R energy levels and wave functions are performed that include explicitly, as fully coupled, all three translational and the two rotational degrees of freedom of the hydrogen molecule, while the cage is taken to be rigid. In addition, the ground-state properties, energetics, and spatial distribution of one and two *p*-H₂ and *o*-D₂ molecules in the large cage are calculated rigorously using the diffusion Monte Carlo method. These calculations reveal that the low-energy T–R dynamics of hydrogen molecules in the large cage are qualitatively different from that inside the small cage, studied by us recently. This is caused by the following: (i) The large cage has a cavity whose diameter is about twice that of the small cage for the hydrogen molecule. (ii) In the small cage, the potential energy surface (PES) for H₂ is essentially flat in the central region, while in the large cage the PES has a prominent maximum at the cage center, whose height exceeds the T–R zero-point energy of H₂/D₂. As a result, the guest molecule is excluded from the central part of the large cage, its wave function localized around the off-center global minimum. Peculiar quantum dynamics of the hydrogen molecule squeezed between the central maximum and the cage wall manifests in the excited T–R states whose energies and wave functions differ greatly from those for the small cage. Moreover, they are sensitive to the variations in the hydrogen-bonding topology, which modulate the corrugation of the cage wall.

I. Introduction

Clathrate hydrates are a large group of inclusion compounds consisting of a framework formed by hydrogen-bonded water molecules where guest molecules are trapped inside the polyhedral cavities.¹ Several years ago, clathrate hydrates with hydrogen molecules as guests were synthesized under very high pressures and low temperatures, typically 180–220 MPa at around 249 K.² They have the classical structure II (sII), comprised of 16 pentagonal dodecahedron (5¹²) small cages and 8 hexakaidecahedron (5¹²6⁴) large cages per unit cell. The small and the large cage are formed by 20 and 28 H₂O molecules, respectively. Initial estimate was that two H₂ molecules occupy the small 5¹² cage, while four H₂ molecules occupy the large 5¹²6⁴ cage,² suggesting that the hydrogen hydrate might be a promising hydrogen storage material.^{3–5} This has motivated numerous further studies of pure H₂^{6,7} and binary clathrate hydrates.^{8–13} Neutron diffraction experiments on the pure sII hydrogen hydrate⁶ found only one D₂ molecule in the small cage and up to four D₂ molecules in the large cage. Single occupancy of D₂ in the small cage was shown also for the binary sII clathrate hydrate with tetrahydrofuran (THF) as the second guest in high-resolution neutron diffraction experiments¹¹ and the hydrogen-storage capacity studies.¹²

A number of theoretical investigations of the pure H₂^{14–19} and the binary H₂–THF clathrate hydrate²⁰ have been reported. Their main focus was on the thermodynamic stability of the clathrates with different number of H₂ molecules in the small and large cages. The treatment of the dynamics of the encapsulated hydrogen molecules has been limited to classical simulations. In only one instance,¹⁶ the problem of H₂ inside the small dodecahedral cage was treated by solving the textbook one-dimensional (1D) Schrödinger equation for the bound states of a structureless particle in a spherically symmetric potential.

The dynamics of one or more hydrogen molecules confined inside the clathrate cage, large or small, is highly quantum mechanical. Therefore, its quantitative description demands solving numerically exactly the multidimensional Schrödinger equation for the coupled translation–rotation (T–R) motions of the guest molecules. The intriguing problem of the quantum dynamics of a hydrogen molecule in confined geometries has to date been investigated only for *para*- and *ortho*-H₂ on amorphous ice surfaces using quantum Monte Carlo simulations²¹ and for H₂ within carbon nanotubes by means of quantum four-dimensional (4D) calculations.^{22–24}

We have initiated a program of systematic and rigorous theoretical investigations of the quantum dynamics of hydrogen molecules inside the small and large cages of sII clathrate hydrate. It allows us to simultaneously address issues of direct experimental relevance and to explore fundamental properties

* To whom correspondence should be addressed. E-mail: zlatko.bacic@nyu.edu.

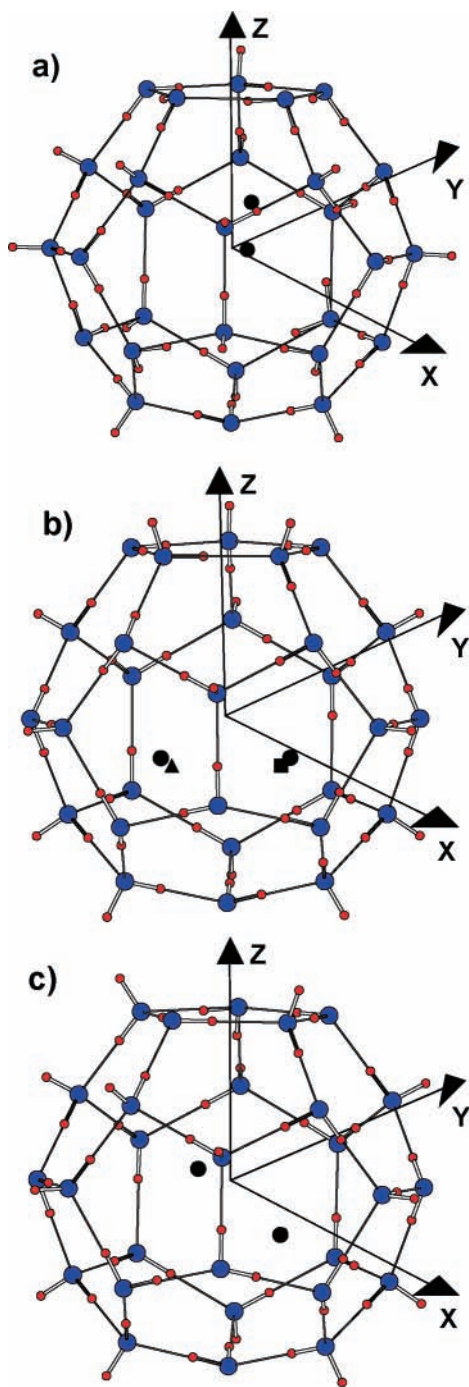


Figure 1. The large hexakaidecahedral ($5^{12}6^4$) cage with one and two hydrogen molecules in their equilibrium configurations. Panels a–c show three different hydrogen-bonding arrangements, referred to in the text as large cages 1, 2, and 3, respectively. The Cartesian X, Y, Z coordinate axes coincide with the three principal axes of the cage; their origin is at the center of mass of the cage. The black circles correspond to the minimum-energy configurations of two hydrogen molecules (their centers of mass). The black triangle and the square in panel b mark the global and the first local minimum, respectively, for one hydrogen molecule; they are not shown in panels a and c because of the almost complete overlap with the black circles. For further details, see the text.

of highly quantum clusters confined in cavities of different shapes and sizes. In the initial publication²⁵ (paper I), we presented the first quantum five-dimensional (5D) calculations of the T–R eigenstates of a single H_2 molecule inside the small dodecahedral (5^{12}) cage, which for the first time provided a quantitative picture of the quantum T–R dynamics of the guest

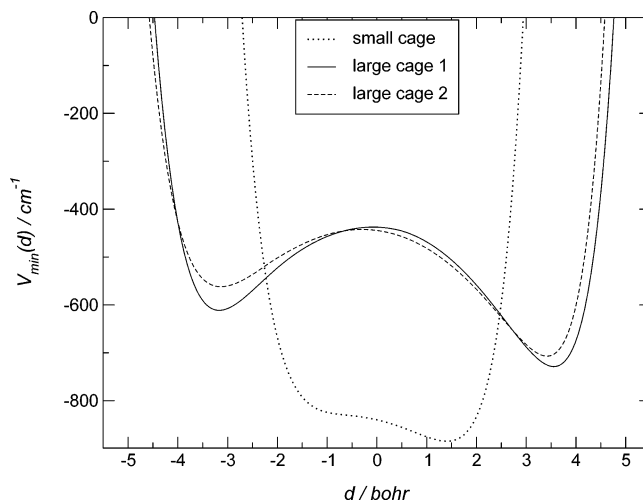


Figure 2. One-dimensional cuts through the 5D PESs of H_2 in the small cage and in the large cages 1 and 2. The potential profiles shown are plotted along the lines that connect the global minima of the PESs with the center of the cages. Their slight asymmetry is caused by the configurational disorder of the H atoms of the framework water molecules.

molecule. The second paper²⁶ (paper II) extended these calculations to a D_2 molecule in the small cage. In addition, energetics and vibrationally averaged structural information were calculated rigorously for one, two, and three *p*- H_2 and *o*- D_2 molecules in the small cage, using the diffusion Monte Carlo (DMC) method.

In this paper, our investigations turn to the large hexakaidecahedral ($5^{12}6^4$) cage. Accurate quantum 5D calculations of T–R energy levels and wave functions are performed for a single H_2 and D_2 molecule inside the large cage, utilizing the methodology described in papers I and II. Moreover, the ground-state properties of one and two *p*- H_2 and *o*- D_2 molecules in the large cage are calculated rigorously using the DMC method. These results depict a quantum T–R dynamics of the guest hydrogen molecules that is qualitatively different from that in the small cage.

II. Theory

In this work, the large cage and the trapped hydrogen molecule(s) are taken to be rigid, while the quantum dynamics of the coupled translational and rotational motions of the guest molecules is treated rigorously. The same approach was taken in our earlier studies of the T–R dynamics of hydrogen molecules in the small cage.^{25,26} The positions of the O atoms of the framework water molecules comprising the large (and small) cage have been determined in the X-ray diffraction experiments.²⁷ The 28 O atoms occupy the corners of the hexakaidecahedron ($5^{12}6^4$) shown in Figure 1, which has 12 pentagonal and 4 hexagonal faces. There is a hydrogen atom of a water molecule on each edge of the cage, but these H atoms are configurationally disordered. The clathrate hydrate cages follow the Euler formula $F + V - E = 2$, where F , V , and E represent the number of faces, vertices, and edges, respectively. Since $F = 16$ and $V = 28$ for the large $5^{12}6^4$ cage, the number of edges (E) is 42. Consequently, 14 of the 28 water molecules must be double donors with both of their H atoms participating in the hydrogen bonds with two neighboring O atoms. The remaining 14 water molecules are single donors, having only one H atom in a hydrogen bond, while the second O–H bond of the molecule is free. The number of possible hydrogen-bonding arrangements exceeds 30 000 for the small 5^{12} cage²⁸ and is undoubtedly much greater for the large $5^{12}6^4$ cage. Three

TABLE 1: Ground-State Energies $E_{0,n}$ of $n = 1, 2$ p -H₂, and o -D₂ Molecules Inside Large Cages 1–3 from the Quantum Dynamics Calculations^a

large cage	large cage 1		large cage 2		large cage 3	
	$n = 1$	$n = 2$	$n = 1$	$n = 2$	$n = 1$	$n = 2$
$E_{0,n}$	-519.76 (-561.42)	-1004.50 ± 0.18 -1095.78 ± 0.14	-494.95 (-526.67)	-938.02 ± 0.16 -1025.20 ± 0.14	-502.64 (-537.48)	-1401.35
$V_{min,n}$	-728.83	-1450.24	-706.98	-1407.12	-719.75	
ZPE_n	209.07 (167.41)	445.74 (354.46)	212.03 (180.31)	469.10 (381.92)	217.11 (182.27)	
$ZPE_n/ V_{min,n} $	0.29 (0.23)	0.31 (0.24)	0.30 (0.26)	0.33 (0.27)	0.30 (0.25)	

^a Also shown are the global minima $V_{min,n}$, the zero-point energies of the coupled translational and rotational motions ZPE_n , obtained as the difference $E_{0,n} - V_{min,n}$, and the ratios $ZPE_n/|V_{min,n}|$. For all the quantities shown, the numbers in parentheses refer to o -D₂. All energies are in cm^{-1} .

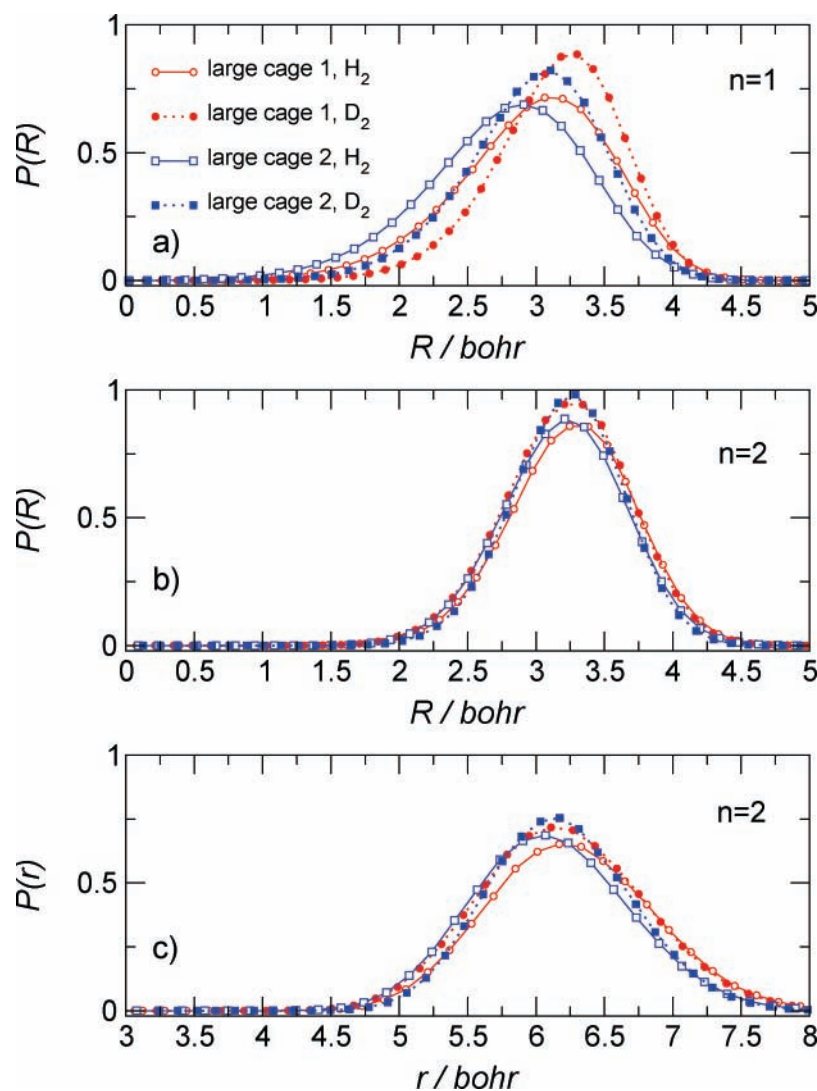


Figure 3. The cage center to p -H₂/ o -D₂ center-of-mass distance (R) probability distribution $P(R)$ for (a) one p -H₂/ o -D₂ molecule and (b) two p -H₂/ o -D₂ molecules. The p -H₂- p -H₂ and o -D₂- o -D₂ center-of-mass distance (r) probability distributions $P(r)$ for two p -H₂ and two o -D₂ molecules, respectively, in large cages 1 and 2 are shown in (c).

different hydrogen-bonding arrangements are displayed in Figure 1. Figure 1a will be referred to as large cage 1 (LC1), Figure 1b as large cage 2 (LC2), and Figure 1c as large cage 3 (LC3). Large cages 1–3 have a different number of nearest-neighbor pairs of water molecules that both have a free, dangling O–H bond, 7 in LC1, 4 in LC2, and 5 in LC3. This topological characteristic correlates with the relative energies of various hydrogen-bonding arrangements in the cubic (H₂O)₈ and dodecahedral (H₂O)₂₀ clusters.²⁸

The potential energy surface (PES) for n hydrogen molecules inside the large cage has the form given in our previous studies

of one and two H₂/D₂ molecules in the small cage.^{25,26} All interactions, among n confined hydrogen molecules (when $n > 1$), as well as those between the guest molecules and the framework H₂O molecules, are assumed to be pairwise additive. For the pair interaction between H₂ and H₂O, the high-quality ab initio 5D (rigid monomer) PES for the H₂–H₂O complex²⁹ is used, whose global minimum is at -240.8 cm^{-1} . The H₂–H₂ pair potential is described by an ab initio 4D (rigid monomer) PES;³⁰ its global minimum lies at -40.00 cm^{-1} .

The 5D T–R energy levels and wave functions of a single H₂/D₂ molecule inside the large cage are calculated as fully

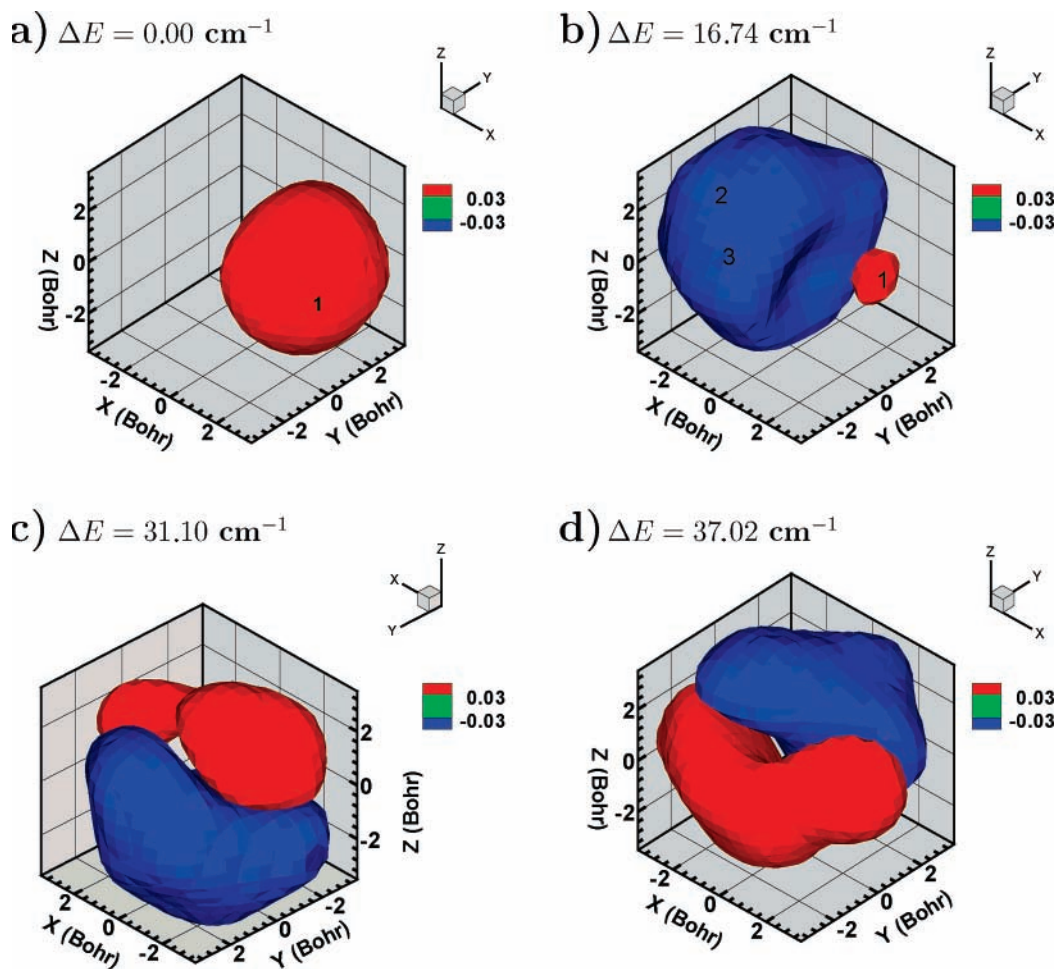


Figure 4. The 3D isosurfaces of the translational parts of the wave functions of the ground state and first three excited states of p -H₂ in large cage 1. The excitation energies ΔE relative to the ground state are shown as well.

coupled using the approach presented in papers I and II. The set of five coordinates (x, y, z, θ, ϕ) is employed; $x, y,$ and z are the Cartesian coordinates of the center of mass (c.m.) of the hydrogen molecule, while the two polar angles θ and ϕ specify its orientation. The origin of the coordinate system is at the c.m. of the cage, and its axes are aligned with the principal axes of the cage. The computational methodology relies on the three-dimensional (3D) direct-product discrete variable representation (DVR)^{31,32} for the $x, y,$ and z coordinates and the spherical harmonics for the angular, $\theta,$ and ϕ coordinates. The sequential diagonalization and truncation procedure^{31,33,34} is utilized to reduce drastically the size of the final Hamiltonian matrix without loss of accuracy. Diagonalization of this truncated Hamiltonian matrix yields the 5D T-R energy levels and wave functions. The dimension of the sine-DVR basis was 50 for each of the three Cartesian coordinates, and its grid spanned the range $-5.10 \text{ au} \leq \lambda \leq 5.10 \text{ au}$ ($\lambda = x, y, z$). The angular basis included functions up to $j_{\text{max}} = 5$. The energy cutoff parameter for the intermediate 3D eigenvector basis³⁵ was set to $680\text{--}880 \text{ cm}^{-1}$ for H₂ and $350\text{--}450 \text{ cm}^{-1}$ for D₂, resulting in the final 5D Hamiltonian matrix of dimension $\sim 14000\text{--}20000$ for H₂ and $\sim 15000\text{--}19000$ for D₂.

The ground-state properties of two hydrogen molecules (treated as rigid), p -H₂ or o -D₂, in the large cage are calculated rigorously for the PESs employed using the DMC method pioneered by Anderson,^{36,37} as we have done previously for 1–3 hydrogen molecules in the small cage.²⁶ Our implementation of the DMC methodology has been discussed already.^{38,39} The rotational constants used in our calculations, DMC and quantum

5D, are $B_{\text{H}_2} = 59.322 \text{ cm}^{-1}$ and $B_{\text{D}_2} = 29.904 \text{ cm}^{-1}$.^{40,41} The vibrationally averaged spatial distribution of p -H₂ and o -D₂ molecule(s) is characterized by means of the probability distribution functions (PDFs) of the following two coordinates: \vec{R}_i , the vector connecting the c.m. of the cage with the c.m. of the i th H₂ molecule, and \vec{r}_{ij} , the vector connecting the centers of mass of H₂ molecules i and j (for $n > 1$). The corresponding 1D PDFs $P(R)$ and $P(r)$, together with the 3D PDF of the Cartesian coordinates of the centers of mass of hydrogen molecules, $P(x, y, z)$, have been defined in paper II. The DMC calculations reported here use an ensemble of 1500 walkers and the time step of 1.0 au. The simulations involve ten independent runs. In every run, after the initial equilibration the ensemble is propagated in 120 blocks consisting of 2000 steps each.

III. Results and Discussion

Figure 2 shows 1D cuts through the 5D PESs for H₂ in large cages 1 and 2 and in the small cage, plotted along the lines connecting the global minima of the PESs with the centers of the cages. These 1D potential profiles are obtained by minimizing the H₂ cage interactions with respect to the angular coordinates θ and ϕ of the H₂ molecule at every position of its center of mass. They make it clear that (i) the large cage has the cavity whose diameter is almost twice that of the small cage, and (ii) that the PESs for H₂ in the two cages have qualitatively different shapes. For the small cage, the PES is rather flat in the central region. In contrast, the PES of H₂ inside the large

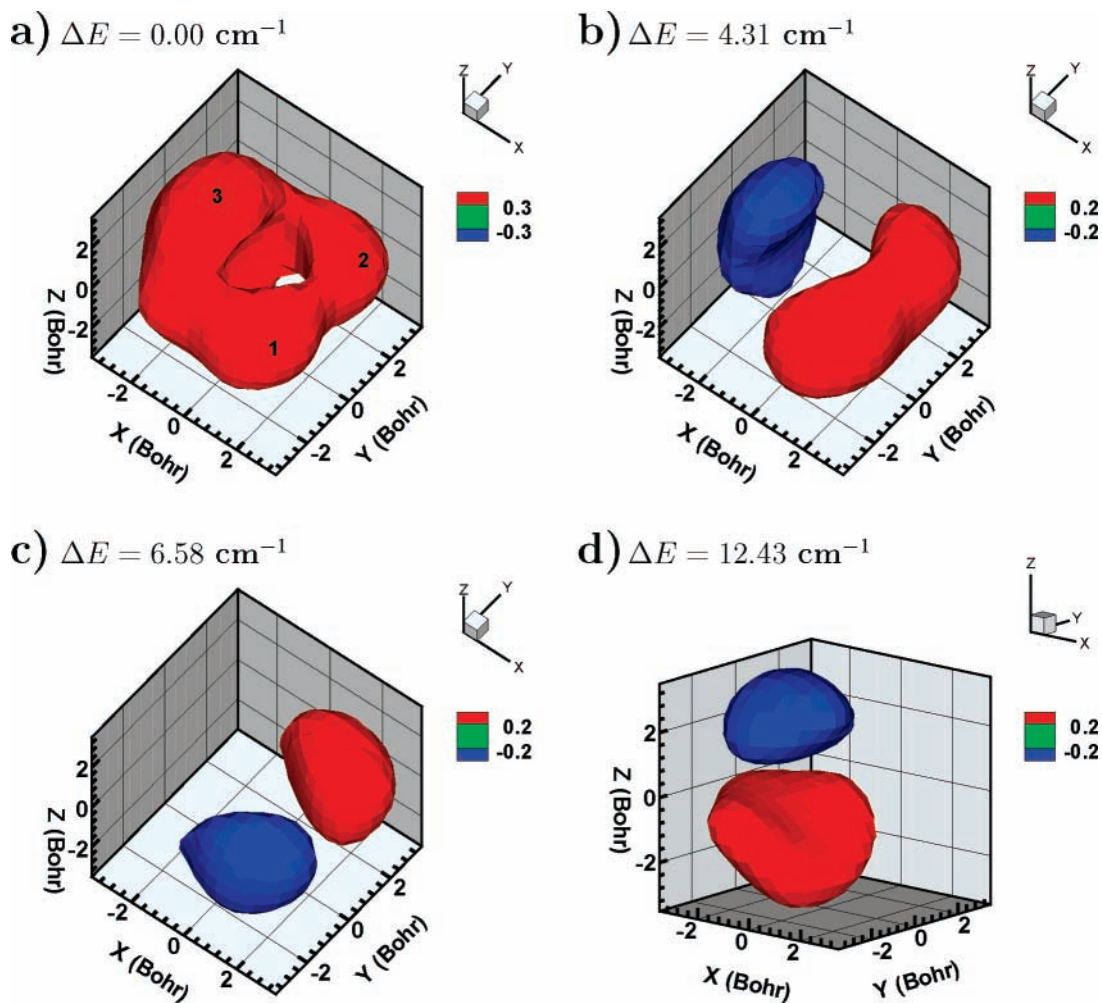


Figure 5. The 3D isosurfaces of the translational parts of the wave functions of the ground state and first three excited states of p -H₂ in large cage 2. The excitation energies ΔE relative to the ground state are shown as well.

cage has a prominent maximum at the cage center, lying ~ 260 – 290 cm^{-1} above the off-center global minimum, depending on the cage. Its presence exerts a major influence on the T–R dynamics of a hydrogen molecule inside the large cage and causes it to be very different from that in the small cage.^{25,26}

Two distinct 1D potential profiles for LC1 and LC2 in Figure 2 show that different hydrogen-bonding topologies give rise to visible differences in the interactions between the guest hydrogen molecule and the cage; for LC3 displayed in Figure 1c, the corresponding profile falls between the other two. The height of the maximum of the PES at the cage center relative to the off-center global minimum is 291.1 cm^{-1} for LC1 and 262.4 cm^{-1} for LC2. For $n = 1$ and 2, the global minima $V_{\text{min},n}$ of large cages 1–3 are listed in Table 1; their well depths vary by about 3% for the three hydrogen-bonding arrangements.

Figure 1 illustrates another interesting feature of hydrogen molecules occupying the large cage. In the global minimum for $n = 2$, the positions of the two hydrogen molecules are very close to the coordinates of the global and the first local minima, respectively, of a single encapsulated H₂. For this reason, Figure 1a,c displays only the $n = 2$ minimum-energy configurations for LC1 and LC3, respectively. In the case of LC2, it is possible to show in Figure 1b the global minimum for $n = 2$ as well as the global and the first local minima for $n = 1$, due to the slight difference of their coordinates. Weak interaction between the two guest molecules at the equilibrium distance of ~ 6.5 bohr is evident also from the observation that the energy of the global minimum for $n = 2$ is almost equal to the sum of

the energies of the global and the first local minima for $n = 1$. For example, for LC1 the energies of the global and the first local minima, -728.83 and -705.33 cm^{-1} , respectively, add up to -1434.16 cm^{-1} , while the $n = 2$ global minimum lies at -1450.24 cm^{-1} . The difference of about -16 cm^{-1} is due to the H₂–H₂ interaction. This is unlike the situation in the small cage²⁶ where the two H₂ molecules are compressed to a significantly shorter intermolecular distance of ~ 4.85 bohr, and their interaction is strongly repulsive.

The equilibrium structures do not include the effects of the zero-point energy (ZPE) of the T–R motions, wave function delocalization, and T–R mode couplings, which are large in this system. A much more complete description is afforded by the rigorous quantum dynamics calculations for one and two H₂/D₂ molecules inside the large cage. Molecular hydrogen exists in two species, even- j ($j = 0, 2, 4, \dots$) *para*-H₂ and *ortho*-D₂, and odd- j ($j = 1, 3, \dots$) *ortho*-H₂ and *para*-D₂. The ground-state energies $E_{0,n}$ of (p -H₂) _{n} and (o -D₂) _{n} , $n = 1$ and 2, in large cages 1–3, are listed in Table 1. The values listed for $n = 1$ are from the quantum 5D calculations (the DMC results are in excellent agreement), while those for $n = 2$ were computed using the DMC method. The ground-state energies of p -H₂ range from -519.8 (LC1) to -495.0 cm^{-1} (LC2), a variation of about 5% for the three hydrogen-bonded topologies. For $n = 2$, the calculated ground-state energies, -1004.5 (LC1) and -938.0 cm^{-1} (LC2) differ by $\sim 7\%$. The ground-state energies of (o -D₂) _{n} , $n = 1$ and 2, exhibit comparable variations over the

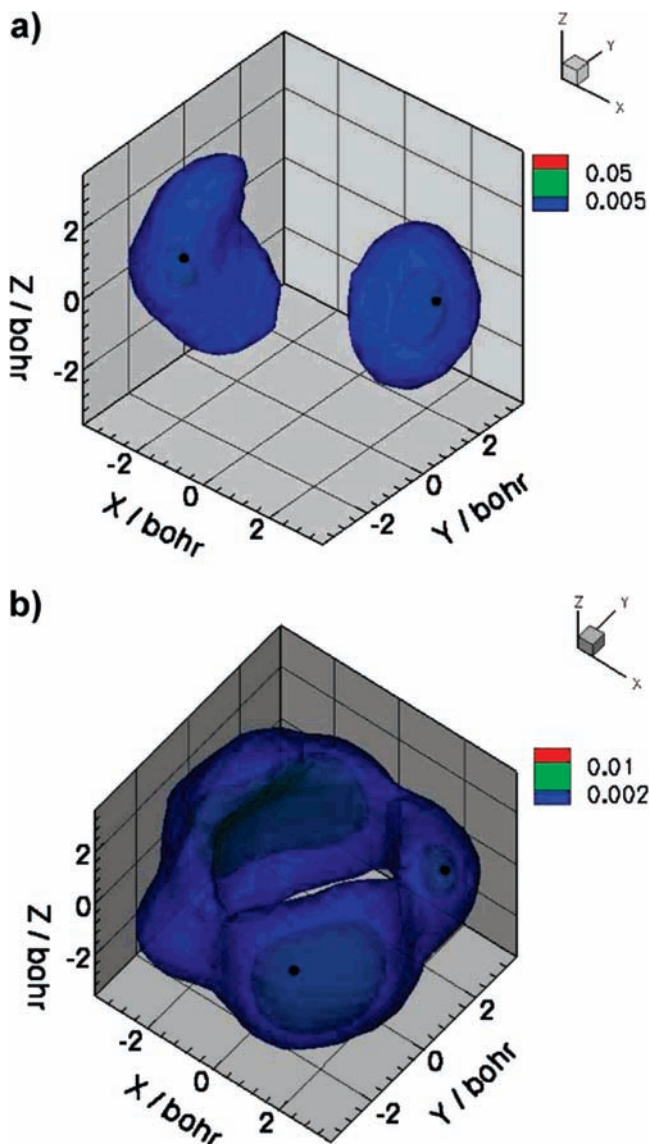


Figure 6. Three-dimensional p -H₂ center-of-mass probability distribution $P(x, y, z)$ of two p -H₂ molecules in large cage 1 (a) and large cage 2 (b). The black dots correspond to the minimum-energy configurations of the two hydrogen molecules (their centers of mass).

large cages 1–3. The explanation for these observations is offered below.

The quantum-mechanical results in Table 1 reveal also that the T–R dynamics of one and two hydrogen molecules inside the large cage differ qualitatively from those in the small cage. First, we notice that the ZPE of one p -H₂ (o -D₂) in large cages 1–3, 209.1–217.1 cm⁻¹ (167.4–182.3 cm⁻¹), is ~20% larger than the ZPE of p -H₂ (o -D₂) inside the small cage,^{25,26} 177.2 cm⁻¹ (144.2 cm⁻¹). This may seem counterintuitive; if the large cage were merely a scaled up version of the small cage, the opposite would be expected. But, as discussed above, the PES of H₂ in the large cage has a prominent maximum at the cage center; this feature is not present in the small cage. The ZPEs of p -H₂ and o -D₂ inside the large cage are much smaller than this potential maximum lying 260–290 cm⁻¹ above the global minimum. Consequently, the guest molecule is confined to the neighborhood of the global minimum, ~3.4–3.6 bohr off the center, which results in the relatively large ZPE. The off-center wave function localization in the large cage is evident in Figure 3a, which shows $P(R)$ for $n = 1$, in the ground state. For p -H₂, $P(R)$ peaks at $R \sim 3.1$ (LC1) and ~2.9 bohr

(LC2). These R values are smaller than those of the global minima of LC1 and LC2, 3.56 and 3.42 bohr, respectively, due to the wave function tunneling into the higher-energy region of the PES at smaller values of R . For o -D₂ in LC1 and LC2, $P(R)$ peaks at larger R values, because its wave function cannot penetrate closer to the cage center as well as that of p -H₂.

Inside the small cage, the ground-state $P(R)$ of p -H₂/ o -D₂ has the maximum at the much smaller value of $R \sim 1.2$ bohr,²⁶ because nothing prevents the molecule from reaching the center of the cage; $P(R)$ goes to zero there simply because of the vanishing volume element.

For the guest molecule whose wave function is localized close to the wall of the large cage, its interior surface is rough, or corrugated. The corrugation depends slightly on the hydrogen-bonding configuration, which accounts for the sensitivity of the ground-state energies and ZPEs to the hydrogen-bonding topology. This sensitivity extends to the low-lying excited T–R eigenstates. By projecting them on the rotational basis, we established that those of p -H₂ are pure (98–99%) $j = 0$ states, while the o -H₂ eigenstates are pure (>99%) $j = 1$ states. The translational parts of the wave functions of the four lowest ($j = 0$) T–R states of p -H₂ in LC1 and LC2 are displayed in Figures 4 and 5, respectively. The translational wave functions in the two cages are very different, and so are the energies of the states. For LC1, the ground and the first excited states are essentially two isomers separated in energy by 16.7 cm⁻¹, with H₂ localized in the ground and the first local minimum of the PES, respectively. The ground-state wave function of LC2 is delocalized over the three lowest-lying minima; the hole in its center corresponds to the maximum of the H₂–cage PES. The first excited state, just 4.3 cm⁻¹ higher in energy, extends over the same three minima, but has a nodal plane perpendicular to the x axis. The next two excited states, at $\Delta E = 6.6$ and 12.4 cm⁻¹, have nodal planes perpendicular to the y and z axes, respectively.

The contrast with the small cage is rather striking. There, the first three excited T–R states of p -H₂ are readily assignable as the fundamental translational excitations in the x , y , and z directions, whose frequencies are 52.4, 66.8, and 77.7 cm⁻¹, respectively.²⁵

We mention that at higher energies the dependence of excited T–R states of the large cage on the hydrogen-bonding topology is less pronounced. Thus, the energy difference between the lowest levels of p -H₂ and o -H₂ is 94.3 cm⁻¹ in LC1, 90.4 cm⁻¹ in LC2, and 90.3 cm⁻¹ in LC3. It is always smaller than $2B_{H_2} = 118.64$ cm⁻¹, the separation between the $j = 0$ and $j = 1$ levels of free H₂ in the gas phase, due to the splitting of the triple $j = 1$ degeneracy caused by the anisotropy of the cage environment.^{25,26} This and other aspects of highly excited T–R eigenstates of the large cage will be analyzed in a future publication.

The T–R dynamics of hydrogen molecules confined in the large and small cages differ greatly also in the rate of growth of the ZPE with n . Table 1 shows that for p -H₂ (o -D₂) in LC1, from $n = 1$ to $n = 2$ the total ZPE increases by the factor of 2.1 (2.1), from 209.1 (167.41) to 445.7 (354.5) cm⁻¹; for LC2, this factor is virtually the same, 2.2 (2.1). In the small cage, on the other hand, the second p -H₂ (o -D₂) causes a fivefold increase (4.7 for o -D₂) of the ZPE.²⁶ In the large cage, the ZPE per p -H₂/ o -D₂ molecule for $n = 2$ is ~10% greater than that of the ZPE of a single p -H₂/ o -D₂, while in the small cage the ZPE per p -H₂ (o -D₂) molecule for $n = 2$ is 2.5 (2.3) times larger than the ZPE for $n = 1$. Finally, in the large cage the ZPE is ~30% of the well depth for both 1 and 2 p -H₂ molecules. But in the small

cage, the ratio of ZPE to the well depth jumps from 0.20 for $n = 1$ to 0.82 for $n = 2$.²⁶ These results suggest that the large cage can be occupied by more than two hydrogen molecules (up to four have been observed experimentally⁶), while the small cage cannot.

The large cage is spacious enough for two hydrogen molecules to execute large-amplitude motions without significantly perturbing one another, while the small cage is not. This is borne out by $P(R)$ for $n = 1$ and 2, shown in Figure 3, which have similar shapes and peak around $R \sim 3.1 - 3.2$ bohr. In contrast, for the small cage, the maximum of $P(R)$ shifts from $R \sim 1.2$ bohr for $n = 1$ to $R \sim 2.5$ bohr for $n = 2$.²⁶ The two hydrogen molecules are virtually excluded from the cage center and are as far apart as the small cage allows at the average distance of $r \sim 4.8$ bohr [$P(r)$ for $n = 2$ in paper II]. The large cage gives the two H₂ molecules considerably more room, and the maximum of $P(r)$ is at $r \sim 6.2$ bohr. The crowding of two H₂ molecules in the small cage is evident also from the significantly smaller widths of both $P(R)$ and $P(r)$ relative to their counterparts for the large cage.

A complementary view of the ground-state spatial distribution of hydrogen molecules is provided by the 3D PDF $P(x, y, z)$ of the centers of mass of two p -H₂ molecules inside large cages 1 and 2, displayed in Figure 6. They exhibit different degrees of wave function (de)localization, due to the variation of the potential landscape with the hydrogen-bonding topology, discussed above (and earlier in paper II).

IV. Conclusions

We have reported a rigorous investigation of the quantum T–R dynamics for $n = 1, 2$ H₂ and D₂ molecules inside the large hexakaidecahedral (5¹²6⁴) cage of the sII clathrate hydrate. The cage was taken to be rigid and so were the guest molecules. The analysis of the ground state (for $n = 1, 2$) and low-lying excited T–R eigenstates (for $n = 1$) presented in this paper has revealed that the low-energy dynamics of the coupled translational and rotational motions of the hydrogen molecules confined in the large cage differs profoundly from those inside the small cage, studied by us previously.^{25,26} This is due to two factors: (1) To the hydrogen molecule, the large cage presents a cavity whose diameter is about twice that of the small cage. (2) The PESs for H₂ in the small cage are rather flat in the central region, but in the large cage they have a maximum at the center of the cage, $\sim 260 - 290$ cm⁻¹ above the global minimum. This maximum, which exceeds the ZPE of H₂/D₂, excludes the guest molecule from the central part of the large cage and localizes its wave function in the vicinity of the global minimum, ~ 3.5 bohr away from the center. Squeezing H₂/D₂ between the central maximum and the cage wall gives rise to excited T–R states whose energies and wave function patterns have little resemblance to those calculated for the small cage and that are sensitive to the changes in the hydrogen-bonding topology of the cage. The ratio of ZPE to the well depth in the large cage is ~ 0.3 for both $n = 1, 2$, while in the small cage it increases sharply from 0.2 for $n = 1$ to 0.8 for $n = 2$.^{25,26}

Work is in progress in our group in two directions: fully characterizing the calculated highly excited T–R states of H₂/D₂ in the large cage and extending the DMC calculations to 5 or 6 hydrogen molecules encapsulated in the large cage; the latter will enable direct comparison with the structural information for $n = 4$ from the neutron diffraction experiments.⁶ The results will be reported in the forthcoming publications.

Acknowledgment. Z.B. is grateful to the National Science Foundation for partial support of this research through Grant

CHE-0315508. The computational resources used in this work were funded in part by the NSF MRI Grant CHE-0420870.

References and Notes

- (1) Sloan, E. D. *Clathrate Hydrates of Natural Gases*; Marcel Dekker: New York, 1998.
- (2) Mao, W. L.; Mao, H. K.; Goncharov, A. F.; Struzhkin, V. V.; Guo, Q.; Hu, J.; Shu, J.; Hemley, R. J.; Somayazulu, M.; Zhao, Y. *Science* **2002**, *297*, 2247.
- (3) Mao, W. L.; Mao, H. K. *Proc. Natl. Acad. Sci., U.S.A.* **2004**, *101*, 708.
- (4) Fichtner, M. *Adv. Eng. Mater.* **2005**, *7*, 443.
- (5) Hu, Y. H.; Ruckenstein, E. *Angew. Chem., Int. Ed.* **2006**, *45*, 2011.
- (6) Lokshin, K. A.; Zhao, Y.; He, D.; Mao, W. L.; Mao, H. K.; Hemley, R. J.; Lobanov, M. V.; Greenblatt, M. *Phys. Rev. Lett.* **2004**, *93*, 125503.
- (7) Zhao, Y.; Xu, H.; Daemen, L. L.; Lokshin, K.; Tait, K. T.; Mao, W. L.; Luo, J.; Currier, R. P.; Hickmott, D. D. *Proc. Natl. Acad. Sci., U.S.A.* **2007**, *104*, 5727.
- (8) Florusse, L. J.; Peters, C. J.; Schoonman, J.; Hester, K. C.; Koh, C. A.; Dec, S. F.; Marsh, K. N.; Sloan, E. D. *Science* **2004**, *306*, 469.
- (9) Lee, H.; Lee, J.-W.; Kim, D. Y.; Park, J.; Seo, Y.-T.; Zeng, H.; Moudrakovski, I. L.; Ratcliffe, C. J.; Ripmeester, J. A. *Nature* **2005**, *434*, 743.
- (10) Kim, D. Y.; Lee, H. *J. Am. Chem. Soc.* **2005**, *127*, 9996.
- (11) Hester, K. C.; Strobel, T. A.; Sloan, E. D.; Koh, C. A.; Huq, A.; Schultz, A. J. *J. Phys. Chem. B* **2006**, *110*, 14024.
- (12) Strobel, T. A.; Taylor, C. J.; Hester, K. C.; Dec, S. F.; Koh, C. A.; Miller, K. T.; Sloan, E. D., Jr. *J. Phys. Chem. B* **2006**, *110*, 17121.
- (13) Choi, Y. N.; Yeon, S. H.; Park, Y.; Choi, S.; Lee, H. *J. Am. Chem. Soc.* **2007**, *129*, 2208.
- (14) Sluiter, M. H. F.; Belosludov, R. V.; Jain, A.; Belosludov, V. R.; Adachi, H.; Kawazoe, Y.; Higuchi, K.; Otani, T. *Lect. Notes Comput. Sci.* **2003**, *2858*, 330.
- (15) Patchkovskii, S.; Tse, J. S. *Proc. Natl. Acad. Sci., U.S.A.* **2003**, *100*, 14645.
- (16) Patchkovskii, S.; Yurchenko, S. N. *Phys. Chem. Chem. Phys.* **2004**, *6*, 4152.
- (17) Alavi, S.; Ripmeester, J. A.; Klug, D. D. *J. Chem. Phys.* **2005**, *123*, 024507.
- (18) Inerbaev, T. M.; Belosludov, V. R.; Belosludov, R. V.; Sluiter, M.; Kawazoe, Y. *Comput. Mater. Sci.* **2006**, *36*, 229.
- (19) Lee, J. W.; Yedlapalli, P.; Lee, S. *J. Phys. Chem. B* **2006**, *110*, 2332.
- (20) Alavi, S.; Ripmeester, J. A.; Klug, D. D. *J. Chem. Phys.* **2006**, *124*, 014704.
- (21) Buch, V.; Devlin, J. P. *J. Chem. Phys.* **1993**, *98*, 4195.
- (22) Lu, T.; Goldfield, E. M.; Gray, S. K. *J. Phys. Chem. B* **2003**, *107*, 12989.
- (23) Lu, T.; Goldfield, E. M.; Gray, S. K. *J. Phys. Chem. B* **2006**, *110*, 1742.
- (24) Yildirim, T.; Harris, A. B. *Phys. Rev. B* **2003**, *67*, 245413.
- (25) Xu, M.; Elmatad, Y.; Sebastianelli, F.; Moskowit, J. W.; Bačić, Z. *J. Phys. Chem. B* **2006**, *110*, 24806.
- (26) Sebastianelli, F.; Xu, M.; Elmatad, Y.; Moskowit, J. W.; Bačić, Z. *J. Phys. Chem. C* **2007**, *111*, 2497.
- (27) Mak, T. C. W.; McMullan, R. K. *J. Chem. Phys.* **1965**, *42*, 2732.
- (28) McDonald, S.; Ojamäe, L.; Singer, S. J. *J. Phys. Chem. A* **1998**, *102*, 2824.
- (29) Hodges, M. P.; Wheatley, R. J.; Schenter, G. K.; Harvey, A. H. *J. Chem. Phys.* **2004**, *120*, 710.
- (30) Diep, P.; Johnson, J. K. *J. Chem. Phys.* **2000**, *112*, 4465.
- (31) Bačić, Z.; Light, J. C. *Annu. Rev. Phys. Chem.* **1989**, *40*, 469.
- (32) Mandziuk, M.; Bačić, Z. *J. Chem. Phys.* **1993**, *98*, 7165.
- (33) Bačić, Z.; Light, J. C. *J. Chem. Phys.* **1986**, *85*, 4594.
- (34) Bačić, Z.; Light, J. C. *J. Chem. Phys.* **1987**, *86*, 3065.
- (35) Liu, S.; Bačić, Z.; Moskowit, J. W.; Schmidt, K. E. *J. Chem. Phys.* **1995**, *103*, 1829.
- (36) Anderson, J. B. *J. Chem. Phys.* **1975**, *63*, 1499.
- (37) Anderson, J. B. *J. Chem. Phys.* **1976**, *65*, 4121.
- (38) Jiang, H.; Bačić, Z. *J. Chem. Phys.* **2005**, *122*, 244306.
- (39) Sebastianelli, F.; Elmatad, Y.; Jiang, H.; Bačić, Z. *J. Chem. Phys.* **2006**, *125*, 164313.
- (40) Jankowski, P.; Szalewicz, K. *J. Chem. Phys.* **1998**, *108*, 3554.
- (41) Jankowski, P.; Szalewicz, K. *J. Chem. Phys.* **2005**, *123*.